Journal of Electronic Research and Application, 2026, Volume 10, Issue 3
http://ojs.bbwpublisher.com/index.php/JERA
ISSN Online: 2208-3510
ISSN Print: 2208-3502

Sub-Pixel-Level Visual Inspection System for Dimensional Measurement of Ceramic Insulators Based on Halcon: Design and Implementation

Yuehua Cao*, Jiajie Han, Hanyang Zhu, Ge Yuan
Information Engineering College, Hangzhou Dianzi University, Hangzhou 311305, China

**Author to whom correspondence should be addressed.*

Abstract: Aiming at the problems of low efficiency, poor accuracy consistency, and reliance on empirical judgment in the manual dimension inspection of ceramic insulators during the production process, a sub-pixel-level visual inspection system based on the Halcon platform was designed. Taking the 95-porcelain insulators with a 60 × 60 specification as the research object, a three-layer inspection architecture of "hardware acquisition–software processing–data output" was constructed. Through key technologies such as camera calibration, distortion correction, sub-pixel contour extraction, and template matching, the automatic measurement of three core dimensions of the insulator, namely height, width, and shed distance, was achieved. The experimental results show that the detection error of this system is controlled within the range of 0.5–1.2mm, the detection success rate reaches 99.2%, the detection time per sample is 2s, and the efficiency is 40% higher than that of traditional manual inspection. It can accurately meet the dimension inspection requirements of "GB/T 772-2005 Technical Conditions for Porcelain Insulators for High-voltage Overhead Lines". This system requires no human intervention, and the detection results are stable and reliable. It provides an efficient solution for the on-line quality control in the production process of ceramic insulators and has important engineering application value.

Keywords: Ceramic insulators; Machine vision; Halcon; Sub-pixel detection; Calibration method; Dimension measurement; Distortion correction; PLC control; Zhang Zhengyou

Online publication: April 22, 2026

1. Introduction

As a core insulating component in power systems, the dimensional accuracy of ceramic insulators directly

determines their insulating performance and installation compatibility, which must strictly comply with the requirements for nominal dimension deviations. Currently, manual caliper measurement is widely adopted by small and medium-sized manufacturing enterprises, and this method has three prominent pain points as follows:

(1) The detection efficiency is extremely low, where measuring a single sample takes more than 30 seconds, which is difficult to keep up with the rhythm of large-scale continuous production;

(2) The accuracy consistency is poor: Manual operations are highly susceptible to subjective factors (such as operator experience and fatigue), leading to significant fluctuations in measurement errors;

(3) The labor intensity is high: Long-term repetitive measurement tasks are prone to causing operator fatigue, which in turn increases the risk of misjudgment [1].

Existing research on ceramic insulators mainly focuses on the optimization of material properties and the detection of surface defects, while studies on high-precision online detection technology for core dimensions during the production process are relatively insufficient. For instance, the machine vision detection method proposed by Bai *et al.* focuses on surface defect identification and does not involve the quantitative measurement of key dimensions of ceramic insulators [2–4]. In addition, the ceramic defect detection algorithms proposed by Guang *et al.* are difficult to be directly applied to the dimension extraction of insulators with umbrella-shaped and irregular structures, failing to meet the requirements of high-precision measurement. Based on the above-mentioned problems, this study takes 95-porcelain insulators as the research object and develops a sub-pixel-level visual inspection system based on the Halcon platform [5]. By integrating the Zhang Zhengyou calibration method and sub-pixel contour extraction technology, the system effectively improves the measurement accuracy, realizes the automatic and high-precision detection of three core dimensions (height, width, and shed distance) of ceramic insulators, and provides reliable technical support for the efficient quality control of ceramic insulator production [6,7].

2. Overall architecture of the visual inspection system

The visual inspection system serves as the core for realizing high-precision dimensional detection of insulators [8,9]. It is required to accurately perform image acquisition, calibration and correction, feature extraction, and dimensional measurement, providing a reliable foundation for classification and decision-making [10]. A visual inspection system featuring a "hardware acquisition–software processing–data output" framework is constructed based on the Halcon platform. Through optimized hardware selection, camera calibration, distortion correction, and the development of dedicated detection algorithms, sub-pixel-level measurement of insulator height, width, and shed spacing is achieved.

In power systems, the dimensional accuracy of ceramic insulators directly affects their insulation performance and installation compatibility. Accordingly, the visual inspection system must achieve a favorable balance between measurement accuracy and real-time performance. The system adopts a three-layer architectural design.

The acquisition layer consists of a Daheng Imaging MER-132-30UC camera, an M1214-MP2 lens, and a ring light source. The camera provides a resolution of 1292×964 pixels with a pixel size of 3.75 μm×3.75 μm. Paired with a 12.325 mm focal-length lens, it achieves an 80 mm×80 mm field of view at a working distance of

275 mm, ensuring full and clear imaging of the insulator.

The processing layer implements core algorithms on the Halcon platform, sequentially performing image preprocessing, camera calibration, distortion correction, feature extraction, and dimensional calculation. Sub-pixel contour extraction and template matching are applied to further improve measurement accuracy.

The output layer transmits detection results, including height, width, shed spacing, and pass/fail status, to the PLC via the TCP/IP protocol in 16-bit binary format. The upper 8 bits store dimensional data, while the lower 8 bits carry the pass/fail flag, guaranteeing efficient and reliable data transmission.

The overall detection workflow focuses on three key dimensions. Height is measured using a one-dimensional gauge to detect edge distances. Shed spacing is obtained by calculating the distance between midpoints after locating the umbrella structure via template matching. Width is derived by fitting a minimum enclosing rectangle to the sub-pixel contour.

Finally, joint development based on Halcon and C# is carried out, and the S7.net library is used to establish Ethernet communication with the PLC, realizing real-time interaction of measurement results. The detailed framework is illustrated in Figure 1.

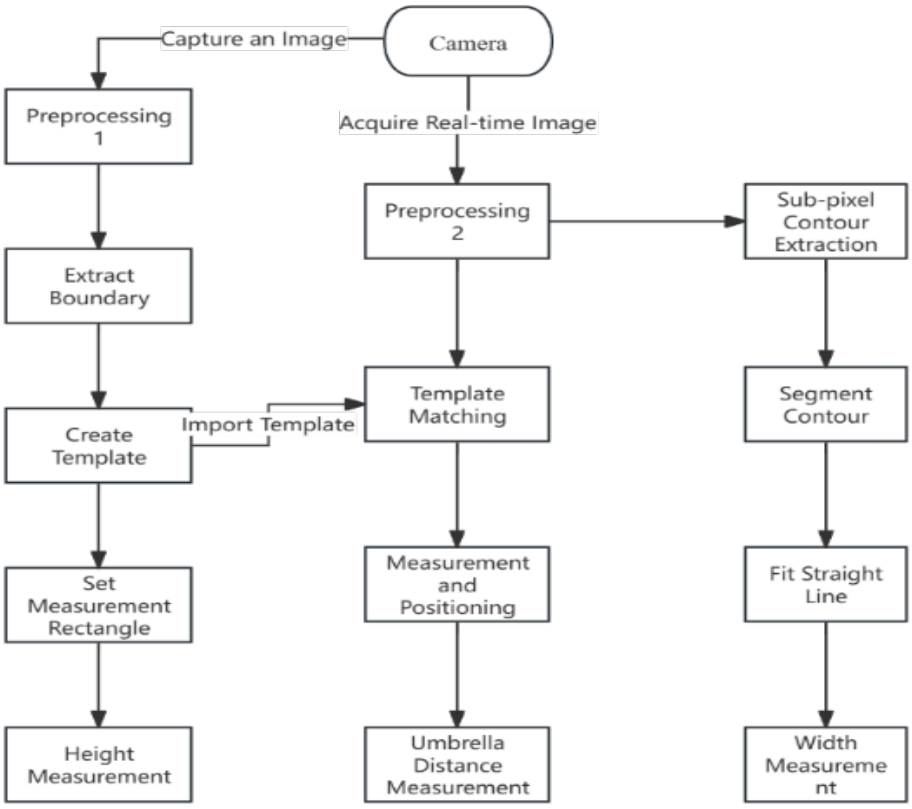

Figure 1. Overall visual inspection framework diagram.

3. Image processing and detection algorithms

3.1. Image pre-processing

Generally, image preprocessing is required prior to formal image processing. After image acquisition,

preprocessing techniques including noise reduction, contrast enhancement, and target feature highlighting are applied to provide a more stable and accurate image foundation for subsequent dimensional measurement [11,12]. Finally, methods such as threshold segmentation and image cropping are adopted to extract the feature region. On the Halcon platform, the specific operation steps are as follows.

First of all, use the built-in Image Acquisition Assistant in Halcon for image acquisition. Locate the "Assistant" option in the Halcon menu bar and select "Open New Image Acquisition" from the drop-down menu.

Then, in the pop-up interface, click "Auto-detect Interface" under the "Resources" section to detect the camera devices recognized by the computer. It should be noted that if the device fails to be detected at this stage, please verify the proper installation of the camera driver. Upon successful recognition of the camera device, click the "Connect" button within the "Connection" panel. In this interface, it can be observed that the color space parameter defaults to "RGB", meaning color images are captured by default.

After completing the aforementioned steps, the acquired images can be viewed in real-time within the image window. The corresponding code for image acquisition is presented below.

Next, the "rgb1_to_gray()" operator is employed to convert the real-time captured images into grayscale. Grayscale processing in image preprocessing serves to simplify the workflow, enhance computational efficiency, and improve robustness against noise. Consequently, it ensures more consistent and stable processing, making it suitable for a majority of computer vision algorithms and image processing pipelines. The visual effect of grayscale conversion is illustrated in Figure 2.

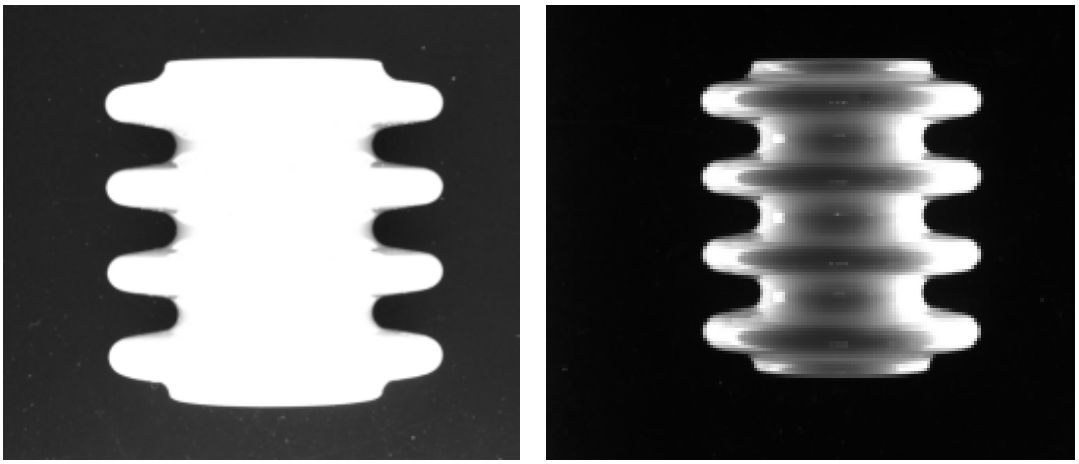

Figure 2. Comparison of photos before and after grayscaling.

After grayscaling, the emphasize() operator is further applied to the image to enhance its high-frequency regions, resulting in a clearer visual effect (Figure 2). This operation helps highlight detailed information in the image and improve its overall visual quality.

Finally, threshold segmentation is performed to partition image pixels into two or more distinct regions, enabling the separation of the detection target from the background. By setting a grayscale threshold, this technique classifies image pixels into two categories: those with grayscale values greater than or equal to the threshold, and those below it. Table 1 presents the parameters and corresponding meanings of the

threshold segmentation operator in Halcon. Halcon uses the threshold() operator as the default for threshold segmentation [13–15]. In this study, a grayscale value of 130 is selected as the threshold; alternatively, the threshold can be adjusted by dragging the dividing line in the histogram, as shown in the grayscale histogram (Figure 3). After applying this operator, the effect of image segmentation is displayed in real time in the image window. As shown in Figure 3, the feature region of the ceramic insulator can be clearly identified. Figure 4 shows the grayscale histogram.

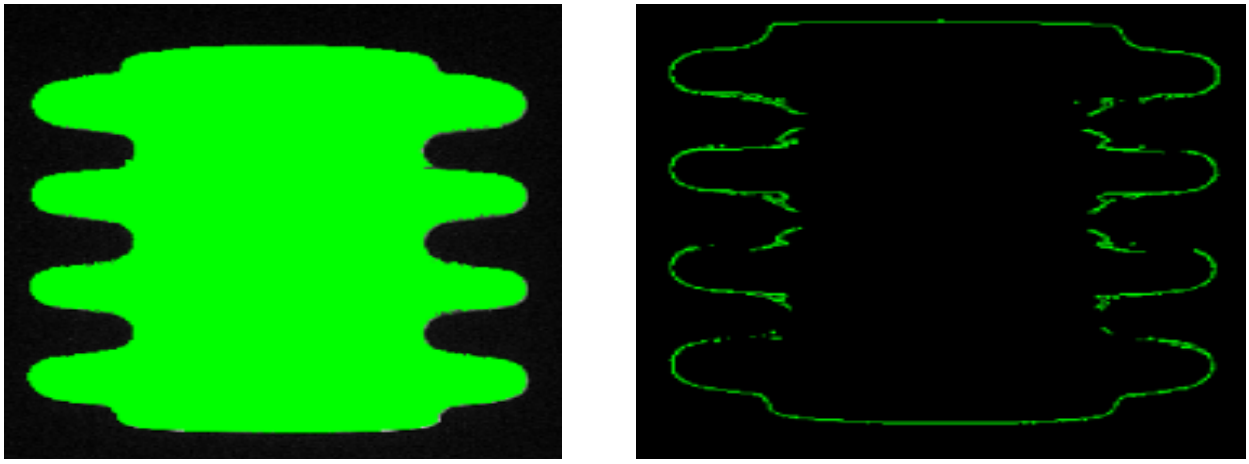

(a) (b)

Figure 3. (a) Effect diagram after enhancement. (b) Feature extraction map.

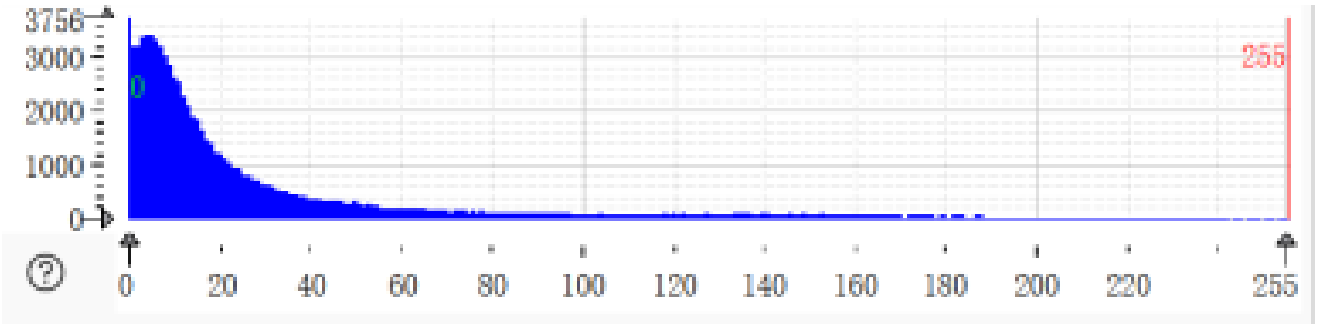

Figure 4. Grayscale histogram.

Table 1. Parameters and meanings of the threshold segmentation operator threshold

Operator	Threshold
Image	Input image
Region	Output region
MinGray	Input minimum grayscale value, range 0–255
MaxGray	Input maximum grayscale value, range 0–255

3.2. Shed distance measurement

After preprocessing to obtain the characteristic image of the porcelain insulator for subsequent analysis, a template must be created for the insulator's edge region. Template matching is then applied to locate the

insulator's edges, enabling the identification of its sheds and the measurement of shed spacing. Prior to template creation, affine transformation is performed on the insulator image to enhance template quality and improve the accuracy of template generation. The workflow for shed spacing measurement is illustrated in Figure 5.

Figure 5. Flowchart of shed distance measurement.

The first step in constructing the shape model is to define the characteristic rectangular region. The gen_rectangle1 function is used to generate a rectangular region, which requires the coordinates of the upper-left and lower-right corners. This rectangle defines the region of interest (ROI). The area_center function is then applied to obtain the center coordinates of the rectangular ROI. As shown in Figure 6 the region enclosed by the red frame is the area used for template creation.

Next, the reduce_domain function is used to extract the image subset corresponding to this rectangular region. The create_shape_model operator is then employed to generate the shape template.

After the template is created, the inspect_shape_model() operator is used to verify the validity and applicability of the template parameters. Finally, the get_shape_model_contours() function is adopted to extract the contour information of the generated model for subsequent matching. The first parameter of this operator is used to store the contour data of the model. The resulting shape template is displayed in Figure 6.

Once the shape model is established, template matching can be performed. It returns the position, rotation angle, and matching score of the matched instances, as illustrated in Figure 7.

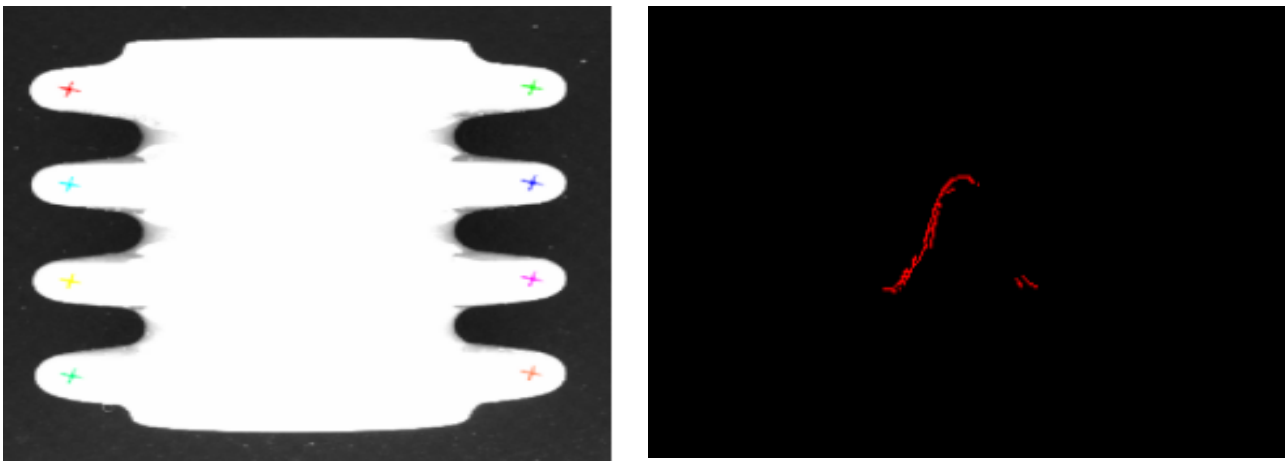

(a) **(b)**

Figure 6. (a) Selecting the rectangular region. (b) Obtained shape template.

Row	[310.606, 237.519, 583.763, 656.77, 795.442, 383.982, 164.194, 726.089]
Column	[426.191, 546.42, 921.965, 800.694, 565.579, 304.749, 670.491, 677.639]
Angle	[0.540347, 0.535126, 3.65263, 3.64463, 3.66435, 0.581627, 0.511377, 3.61969]
Score	[0.998995, 0.989733, 0.988283, 0.983287, 0.963718, 0.962988, 0.959972, 0.908175]

Figure 7. Position information, etc. obtained after matching instances.

3.3. Insulator height measurement

Porcelain insulators exhibit diverse wide-side shapes, which are not always straight but may also include arc- shaped edges. To accommodate such varied edge profiles, a one-dimensional measurement tool is used to perform edge detection along a predefined line. This tool can detect transitions from bright to dark or dark to bright, making it adaptable to different edge types. It effectively handles the special contours of porcelain insulators and enables accurate and efficient height measurement.

First, a measurement object must be generated to define the region to be measured. If measurement is performed along a straight line, the object is defined by a rectangle; if along an arc, the object is defined as an arc segment. In this work, the height of the porcelain insulator is measured along a straight line. Therefore, based on the shed spacing measurement results, a perpendicular line is constructed at the midpoint of the center-point connection line, and this perpendicular line is used as the direction of the measurement line. The gen_ measure_ rectangle2() operator is applied to create a measurement rectangle for height detection. The effect is illustrated in Figure 8.

Then, the measure_pairs() operator is called to extract straight edge pairs perpendicular to the main measurement axis. This operator returns the center position, amplitude, spacing, and distance between adjacent edge pairs. The actual height of the insulator is obtained by calculating the distance between the edge centers of the outermost edge pairs. This approach effectively addresses measurement difficulties caused by arc-shaped edges and guarantees the accuracy of height measurement.

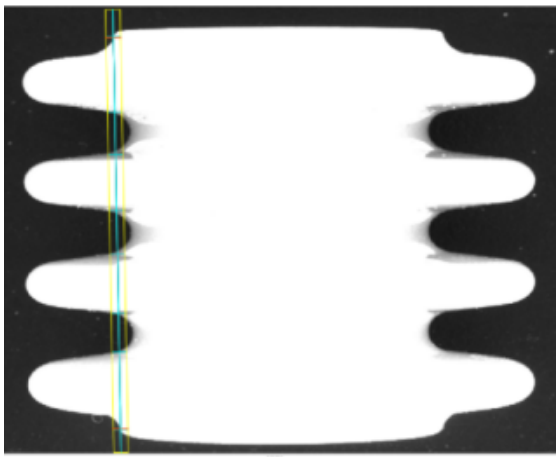

Figure 8. Height-measurement rectangles.

3.4 Insulator width measurement

When measuring the width, the acquired image undergoes reprocessing. In this processing workflow, focus isplaced on the edge region of the porcelain insulator to extract its sub-pixel contour.

Sub-pixel contours offer higher measurement accuracy compared to integer-pixel contours, which is conducive to the precise measurement of the dimensions and shapes of porcelain insulators. The more detailed edge information provided by sub-pixel contours enables more accurate positioning of edge centers, which is also highly beneficial for the high-precision contour positioning of porcelain insulators. Meanwhile, sub-pixel contours are typically smoother when representing curves or curved edges; this helps reduce unnecessary jagged effects caused by image quantization and further improves the accuracy of measurement results.

Prior to width measurement, image preprocessing is still required, which will not be elaborated on herein. After preprocessing, contour extraction is performed. For the cropped image, the edges_sub_pix() operator can be used to extract the outer edge contour of the region at the sub-pixel level. Compared with the edges_image() operator, the edges_sub_pix() operator extracts edges at the sub-pixel level, allowing the output edge positions to lie between the integer coordinates of pixels and thus providing higher positioning accuracy. However, due to the involvement of sub-pixel-level calculations, its computation speed may be slower than that of integer-pixel edge extraction. As shown in Figure 9, the sub-pixel contour of the porcelain insulator's edge is successfully extracted.

The smooth_contours_xld() operator is employed to smooth the contour, resulting in smoother representation of curves and curved edges. This reduces the jagged artifacts caused by image quantization and improves the stability and accuracy of measurement results. The smoothed sub-pixel edge is illustrated in Figure 10.

After obtaining the smooth sub-pixel contour of the porcelain insulator, the shape_trans_xld() operator is used to generate the circumscribed rectangle of the contour, as illustrated in Figure 10.

Then, the coordinates of two nondiagonal points (Row0, Col0) of the circumscribed rectangle are obtained via the get_contour_xld(XLDTrans, Row, Col) operator. The width of the porcelain insulator is determined by calculating the distance between two adjacent shortside vertices of the rectangle.

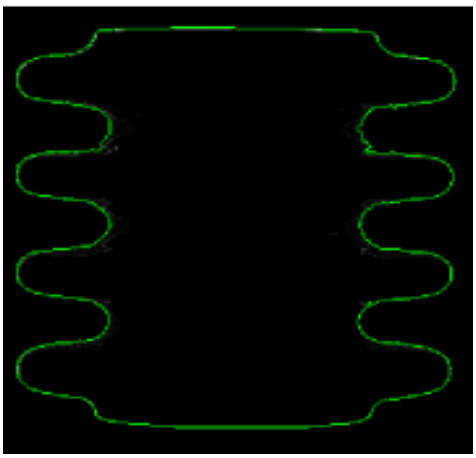

Figure 9. Sub-pixel edge..

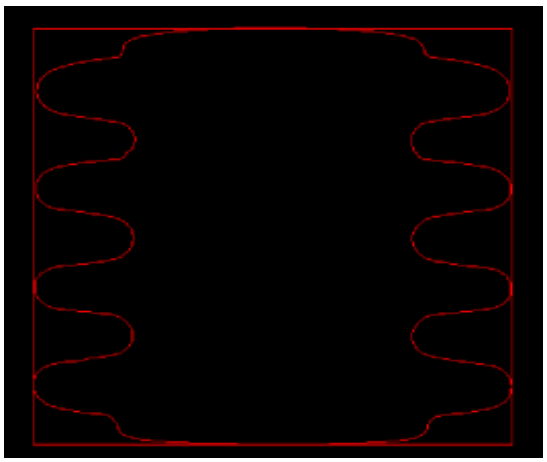

Figure 10. Detection parameters of insulator samples

3.5.Detection results and error analysis

Detection items include height, width, and shed distance. The nominal size of height and width is 60 mm, with average detection values of 60.65 mm and 60.66 mm respectively. The maximum error and minimum error are 1.2 mm and 0.5 mm for height, and 1.1 mm and 0.4 mm for width. The nominal value of shed distance is 15 mm, with an average detection value of 15.80 mm, a maximum error of 1.2 mm, and a minimum error of 0.7 mm.

Compared with the nominal sizes, all measurement errors range from 0.5 mm to 1.2 mm. Among these items, the error of shed distance is larger than that of height and width.

Error analysis shows that the errors of height and width mainly result from the accuracy of camera calibration. The intrinsic and extrinsic parameters of the camera directly determine the mapping relationship between pixel values and actual physical dimensions. The calibration assistant in Halcon was adopted to obtain these parameters, which automatically calculates the camera parameters according to the captured calibration-plate images. Therefore, the quality of the calibration-plate images directly influences the accuracy of the calibration results.

The larger error in shed distance is attributed to the template-matching method used in its measurement. A template is established based on the edge of one shed, and then all sheds are located by template matching to calculate the shed distance. Poor template quality will lead to template deviation, which directly affects the positioning accuracy of sheds and causes a relatively large measurement error.

By optimizing the acquisition of calibration-plate images by adding two oblique-angle images and improving the selection of template regions by avoiding texture-dense areas, the error of shed distance can be reduced to below 0.9 mm.

4. Conclusion

Aiming at the industrial problems of low efficiency, poor consistency, and heavy reliance on manual experience in the dimensional inspection of ceramic insulators during production, this study designs and implements a sub-pixel-level visual inspection system based on the Halcon platform. The system adopts a three-layer architecture: hardware acquisition, software processing, and data output. A Daheng industrial camera, lens, and ring light source are used to achieve clear imaging and reflection suppression. Through Zhang Zhengyou calibration, distortion correction, image preprocessing, template matching, and sub-pixel contour extraction, the automatic measurement of three key dimensions (height, width, and shed spacing) is realized. Experimental results show that the detection error of the system ranges from 0.5 to 1.2 mm, and the average errors fully meet the tolerance requirement of ± 2.0 mm specified in GB/T 772-2005. The inspection time per sample is 1.8 s, improving efficiency by about 40% compared with manual inspection, and the continuous detection success rate reaches 99.2%. The system can replace manual inspection and realize automatic online quality control. To address the issues of illumination sensitivity and relatively large shed spacing error, future work will improve robustness and generality via closed- loop light control, multi-template matching, and deep learning algorithms, with the goal of controlling the overall error within 0.8 mm.

Funding

General Research Project of Education Department of Zhejiang Province (Project No.: Y202558181); Scientific Research Fund of Hangzhou Dianzi University Information Engineering College (Projecy No.: KYP0324006); National Training Program of Innovation and Entrepreneurship for Undergraduates (Project No.: 202513279018); Laboratory Research Project, College of Information Engineering, Hangzhou Dianzi University (Project No.: SYSYJ20250601).

Disclosure statement

The authors declare no conflict of interest.

References

[1] Xiong Y, Shen Y, et al., 2020, Influence of Bolt Size Deviation of Line Porcelain Insulators on Load Value. Hubei Electric Power, 8(4): 53–58.

[2] Chen Z, Zhuang J, Lin J, et al., 2020, Development of Live Detection System for Porcelain Post Insulators. High Voltage Apparatus, 56(7): 212–217.

[3] Wang J, Li J, et al., 2021, Interface Design and Electrical Performance of Composite Gradient Insulation for DC Basin Insulators. Transactions of China Electrotechnical Society, 36(15): 3210–3218.

[4] Zhong Z, Zhang X, et al., 2022, Study on Deterioration Mechanism of Composite Insulator Core Rod Under High Humidity Environment. Proceedings of the CSEE, 42(8): 2987–2996.

[5] Sun R, Wang L, et al., 2020, Influence of Deterioration and Contamination of Porcelain Insulator Strings on Infrared Imaging and Heating Characteristics. High Voltage Engineering, 46(3): 875–883.

[6] Huang Y, Yu X, Ma X, et al., 2020, Study on Bending Resistance of Line Porcelain Insulators. Mechatronics, 2020(1– 2): 52–57.

[8] Meng D, 2018, Design and Analysis of Automatic Cutting Production Line for Ceramic Insulators Based on Robot, thesis, Jiangxi University of Science and Technology.

[9] Jiao E, Du R, 2010, Realization of Industrial Robot Sorting Technology. Control and Measurement, 2010(2): 84–87.

[10] Zhang Y, 2020, Design and Practice of Industrial Robot Sorting System. Electric Engineering, 2020(10): 34–39.

[11] Bai H, 2022, Surface Defect Detection Method of Porcelain Insulators Based on Machine Vision. Automation of Manufacturing Process, 44(5): 123–126.

[12] Wan G, et al., 2021, Improved YOLOv5s for Surface Defect Detection of Ceramic Tiles. Journal of Computational Design and Engineering, 8(3): 1024–1035.

[13] Li H, 2023, Research and Simulation of Material Handling Workstation Based on Industrial Robot. Electronic Components and Information Technology, 7(2): 189–192.

[14] Long Y, Wei W, Shu Y, et al., 2023, Detection Method for Damaged Rotating Insulator Based on Adaptive Key Points. Computer Engineering, 49(9): 272–278.

[15] Liu Y, Jaw D, Huang S, et al., 2018, Context-Aware Deep Network for Snow Removal. IEEE Transactions on

Image Processing, 27(6): 3064–3073.

[16] Liu S, Zhou S, 2024, Research on Insulator Detection Algorithm of High-speed Rail Contact Line. Computer Engineering, 50(5): 200–208.